Modulating Retro-reflectors for Space, Tracking, Acquisition and Ranging using Multiple Quantum Well Technology

G. Charmaine Gilbreath, N. Glenn Creamer, W. S. Rabinovich,
Timothy J. Meehan, Michael J. Vilcheck,
John A. Vasquez, Rita Mahon,[1] Eun Oh, Peter G. Goetz, and Sharon Mozersky

Naval Research Laboratory, Code 7215
http://mrr.nrl.navy.mil

Key Words: MQW Retromodulators, Modulating Retroreflector(s),Inter-spacecraft communications and navigation, space control

Abstract

This paper describes a novel concept for optical interrogation, communication, and navigation between spacecraft platforms. The technique uses a gimbaled laser source on a pursuer spacecraft and an array of solid-state, multiple quantum well modulating retroreflectors on a target spacecraft. The sensor system provides high-bandwidth optical communication, centimeter-level relative positioning, and better than arc-minute-level relative attitude of the target platform with minimal sacrifice in target size, weight, and power. To accomplish the relative navigation, each target retroreflector return is modulated with a unique code sequence, allowing for individual discrimination of the detected composite signal at the pursuer location. Experimental results using a dual-platform, multi-degree-of-freedom testbed provide verification and demonstration of the concept, highlighting its potential for applications such as inter-spacecraft rendezvous and capture, long-baseline space interferometry, and formation flying.

Introduction and Objectives

Due to the benefits of autonomous spacecraft-to-spacecraft interrogation, communication, and navigation for civilian, commercial, and military space missions, there has been a significant amount of research and development on associated relative sensor systems over the past few years.[1-9] These systems typically implement radio- (RF) communication links, GPS sensing for long-range relative positioning, and combinations of visual and laser ranging for short-range proximity operations. Most approaches require the target spacecraft to possess an RF antenna and transmitter along with a GPS sensor to transmit navigational data to the pursuer spacecraft. Additionally, any strategies requiring GPS availability are not suitable for geosynchronous or deep space missions unless a quasi-GPS system is emulated between each vehicle.[10] Although the visual/laser systems provide sufficient accuracy of relative states for close-in operations (i.e. 0 to 50 meters), their mid- to long-range capability (i.e. >50 meters) becomes significantly cruder, with relative position and attitude errors reaching tens of meters and tens of degrees at ranges exceeding 100 meters.

In this paper, we develop and test a novel concept utilizing solid-state multiple quantum well (MQW) modulating retroreflectors to provide inter-spacecraft laser interrogation, communication, and navigation. The modulating retroreflectors enable compact, low power, and low mass optical data transfer on the order of megabits per second,[11] and relative navigation on the order of centimeters in three-axis position and arcminutes in two-axis tilt orientation for this instrumentation. Links over ranges of kilometers down to a few meters are possible. For close proximity operations of about 10 meters or less (docking missions, for example), this concept could work harmoniously with a vision-based system, or possibly be utilized as a single sensor solution with appropriate adaptable optics.

Multiple Quantum Well Modulating Retroreflectors

Modulating retroreflector (MRR) devices utilizing Mutliple Quantum Well (MQW) technology provide a low power, low weight, multi-functional solution to the need to reduce parasitic payload

[1] Author is with Jaycor, Inc., McLean, VA 22102.

Free-Space Laser Communication and Laser Imaging II, Jennifer C. Ricklin, David G. Voelz, Editors, Proceedings of SPIE Vol. 4821 (2002) © 2002 SPIE · 0277-786X/02/$15.00

requirements from conventional communications technologies. An MQW modulating retroreflector is a solid-state device that allows optical communication and ranging between two platforms. MQW shutters are particularly suited to these applications because the technology enables fast data rates, requires very low drive powers, is lightweight, robust, and is not polarization-sensitive.[12.13] The device is also radiation-hard. (See the Naval Research Laboratory's MRR web page at http://mrr.nrl.navy.mil.)

Implementation of such devices requires that only one of the platforms have an onboard laser, telescope, and tracker. Thus, the device is well suited to asymmetric problems in which one platform has a large payload capacity and serves as the pursuer and interrogator and the other platform serves as a probe. The pursuer illuminates the target platform carrying the modulating retroreflectors with a laser beam. The laser beam is automatically reflected back to the pursuer, with no need for target pointing or tracking. The reflected return can be modulated in an On Off Keying (OOK) mode using the MQW solid-state shutters. A representative concept is illustrated in Figure 1.

The modulators must possess several characteristics that enable an efficient link. The shutter must have a high switching speed, low power consumption, large area, wide field-of-view, and high optical quality. In addition, it must work at wavelengths where good laser sources are available, be radiation-tolerant (for space applications) and rugged. Semiconductor multiple quantum well modulators are one of the few technologies that meet all these requirements.[14] A more complete description of the physics of the device is described in the literature and in another paper in this Proceedings. [15]

When a moderate voltage (on the order of 7V-20V) is placed across the device in reverse bias, the absorption feature changes, both shifting in wavelength and changing in magnitude. Thus, the transmission of the device near this absorption feature changes dramatically and can serve as a solid-state on-off shutter. This switching capability is shown in Figure 2 for an InGaAs-based MQW modulator. As shown in the figure, the device demonstrates how the contrast ratio changes as a function of drive voltage for the 980nm device used in these experiments.

Unlike liquid crystal modulators, MQW modulators have very high switching speeds. Small devices (diameters of microns) have been operated at speeds in the tens of GHz. In practice, the speed is limited primarily by the resistance/capacitance (RC) time constant of the device. Thus, the large area devices (on the order of a centimeter) used for retromodulator-based communications typically have speeds between 1 and 10 Mbps. Higher speeds are possible, however, depending on range and the sophistication of the fabrication process. For this effort, we configured the devices to operate at one Mbps.

Data Link Considerations

In practice, except for close ranges, the link (rather than the modulator) limits performance of a modulating retroreflector system. For a conventional corner-cube modulating retroreflector, MQW technology should allow data rates in the tens of megabits per second, depending on the range and the interrogator system. For a diffraction-limited system the optical power, retroreflected from the target platform back to the pursuer platform scales as:

$$\frac{P_{laser} D_{retro}^4 D_{rec}^2 T_{atm}^2}{\theta_{div}^2 \rho^4 \lambda^2} \qquad (1)$$

where P_{laser} is the power of the laser transmitter , D_{retro} is the diameter of the modulating retroreflector on the target or probe, D_{rec} is the diameter of the receive telescope on the pursuer, T_{atm} is the loss due to transmission through the atmosphere, θ_{div} is the divergence of the transmitted laser beam, and ρ is the range between the two platforms.

The strongest dependencies are on the range and the corner-cube retromodulator diameter, both of which scale as fourth powers for diffraction-limited payloads. Conventional retroreflector links fall off more strongly with range than conventional links because of their bi-directional nature.

Target Spacecraft MRR Array

To achieve relative three-axis positional tracking and two-axis tilt orientation on the target, we designed a target board sensor array consisting of eight modulating retroreflectors, as depicted in Figure 3. The center retroreflector (MRR1) and outer three retroreflectors (MRR6, MRR7, MRR8) lie in the same plane and the four inner retroreflectors (MRR2, MRR3, MRR4, MRR5) surrounding the center are canted. In this demonstration, we canted the inner array by 20 degrees. Upon illumination of the entire array by the pursuer laser beam, the

reflected signals from each MRR are uniquely modulated and returned to the pursuer. The intensity or strength of each reflected signal is linearly proportional to the angle of the incoming laser beam relative to the mounted MRR boresight, as shown in the test data of Figure 4. This proportionality is exploited to determine the navigation solution. As described later, the signal intensities from the outer three reflectors are used for laser gimbal tracking control and the signal intensities from the inner five reflectors are used for relative attitude determination.

Pursuer Spacecraft Laser Interrogator, Detector, and Signal Processing Logic

The pursuer spacecraft houses the interrogating gimbaled laser, an analog photodetector, an analog-to-digital converter, and the associated signal processing logic required to transmit the continuous-wave laser beam to the target and receive the reflected, modulated signals from the target MRR array. As depicted in Figure 5, the aggregate return of photons is captured by the analog photodetector and converted to a digital signal through the analog-to-digital converter. Discrimination and isolation of each individual MRR signal is then achieved through a set of matching filters tuned to the unique modulator code sequence associated with each MRR. These signals are then used to determine the relative navigation solution. Additionally, any critical target information can be transmitted to the pursuer by modulating the center MRR base carrier code with the data in binary form.

Inter-Spacecraft Relative Navigation Equations

To determine the target relative navigation solution the pursuer's gimbaled laser is required to detect and track the MRR array as it moves in free space. Initial detection is achieved by performing a series of decreasing rectangular searches in gimbal azimuth and elevation space based on pre-defined signal threshold levels. As the laser beam crosses the MRR array the return signal level will quickly increase until the threshold is reached, initiating a tighter search pattern. This iterative process is continued until a maximum signal level is obtained and all retroreflectors are illuminated. Subsequent gimbal tracking is achieved by equalizing the signal return intensities from the three outer retroreflectors on the target board, resulting in a laser beam that is continually centered on the MRR array.

The notational definitions for inter-spacecraft geometry are depicted in Figure 6. The relative position vector $\vec{\mathbf{R}}$ is determined from the range ρ and the laser beam unit vector $\hat{\boldsymbol{l}}$, yielding

$$\vec{\mathbf{R}} = \rho\hat{\boldsymbol{l}} = \rho\,(\cos\mathrm{EL}\cos\mathrm{AZ}\,\hat{\mathbf{p}}_1 + \cos\mathrm{EL}\sin\mathrm{AZ}\,\hat{\mathbf{p}}_2 + \sin\mathrm{EL}\,\hat{\mathbf{p}}_3) \tag{3}$$

where $\hat{\mathbf{p}}_1$, $\hat{\mathbf{p}}_2$, and $\hat{\mathbf{p}}_3$ are orthogonal unit basis vectors defining the pursuer frame, and AZ and EL are the gimbal azimuth and elevation angles, respectively, measured by the gimbal encoders relative to the pursuer frame. The range measurement to the central retroreflector is determined from time-of-flight (TOF) techniques, similar to the approach used by laser range finders for surveying. The TOF is obtained by measuring the round-trip time it takes a pulse to travel from the laser diode to the retroreflector and back, yielding

$$\rho = \tfrac{1}{2}\,(\mathrm{TOF} * c) \tag{4}$$

where c represents the speed of light.

The relative two-axis attitude (tilt) matrix relating the target frame ***T*** to the pursuer frame ***P*** is determined using a 3-2 Euler angle sequence, yielding

$$\mathbf{C}_{\boldsymbol{T/P}} = \begin{bmatrix} \cos\theta & 0 & -\sin\theta \\ 0 & 1 & 0 \\ \sin\theta & 0 & \cos\theta \end{bmatrix} \begin{bmatrix} \cos\psi & \sin\psi & 0 \\ -\sin\psi & \cos\psi & 0 \\ 0 & 0 & 1 \end{bmatrix} \tag{5}$$

where ψ and θ are relative yaw and pitch tilt angles, respectively. The two tilt angles are derived from the relative signal intensities of each of the five central retroreflectors. For an incoming laser beam at an angle α_i relative to the (i)th MRR boresight, the reflected signal intensity becomes

$$S_i = S_o - m\alpha_i \tag{6}$$

where S_o represents the maximum intensity return if the laser were directly on boresight, and m represents the slope of the straight line given in Figure 4. Adopting the numbering scheme from Figure 3 and uncoupling yaw and pitch motion by assuming relatively small tilt angles (~30 degrees or less), an estimate of these angles becomes

$$\text{IF } S_3 > S_5: \quad \psi = \mathrm{AZ} - \tfrac{1}{2}\frac{S_3 - S_5}{S_1 - S_5}\beta$$

$$\text{ELSE:} \qquad \psi = AZ + \tfrac{1}{2}\frac{S_5 - S_3}{S_1 - S_3}\beta$$

$$\text{IF } S_2 > S_4: \quad \theta = EL - \tfrac{1}{2}\frac{S_2 - S_4}{S_1 - S_4}\beta \qquad (7)$$

$$\text{ELSE:} \qquad \theta = EL + \tfrac{1}{2}\frac{S_4 - S_2}{S_1 - S_2}\beta$$

where β is the known cant angle of the four inner canted reflectors, and it is assumed that the gimbal azimuth and elevation angles are also relatively small such that they are approximately aligned with the pursuer $\hat{\mathbf{p}}_3$ and $\hat{\mathbf{p}}_2$ axes, respectively. It is clear that this differencing strategy eliminates the need for experimentally calibrating the fixed bias S_o and the slope m. Additionally, the intensity-based approach eliminates the need for tedious and precise clock synchronization that would be required of a TOF-based strategy in which the target orientation is determined from the relative ranges to each MRR. Lastly, since the sensitivity of the signal return intensity is directly proportional to the angle off boresight, this strategy is, in principle, independent of range as long as sufficient laser power is available for long range operations (tens of kilometers).

The 5-state navigation solution derived from equations (3) through (7) provides the relative position vector and tilt angles of the target platform. During illumination of the entire MRR array, the relative roll angle about the laser beam unit vector $\hat{\boldsymbol{l}}$ is unobservable since the return signal intensities are insensitive to that angle. In the event of handover to a vision-based camera for close proximity operations such as target capture, this angle would be observable from the vision system after handover is completed. For other mission scenarios, this angle could either be deduced to some coarse level of accuracy from approximately known target dynamics (such as gravity-gradient stabilization) or estimated by traversing the laser beam across the array board and identifying the resulting signal drop-outs.

Experimental Verification Using NRL's Dual-Platform Dynamic Motion Simulator

The Naval Research Laboratory's Dynamic Motion Simulator (DMS) was used for validation and performance evaluation of the inter-spacecraft MRR sensor system for relative communication and navigation. As shown by the photograph in Figure 7, the DMS facility consists of a 6 degree-of-freedom pursuer platform and a 4, soon-to-be six, degree-of-freedom target platform, each driven autonomously and independently using a Pentium III personal computer. The pursuer platform travels in the horizontal plane using an x-y trolley system, and in the vertical direction as well as in three rotational directions (yaw, pitch, and roll) using a robotic manipulator arm. The target platform travels in the horizontal plane using an x-y trolley system, as well as in two rotational directions (yaw and pitch) using a two-axis gimbal mechanism. The repeatable accuracy of the facility is a few millimeters in position and a few arcminutes in rotation, valid over a workspace volume of about 30 x 15 x 3 meters.

For our experiments the pursuer platform was equipped with a gimballed optical transmitter/receive system comprised of a 100mW laser diode operating at a 976 nm , a 10 MHzAvalanche photodetector, a signal amplifier, an analog-to-digital converter, and eight digital matched filters. The optical configuration was monostatic and used a partially transmissive flat for aperture sharing. The configuration is shown in Figure 8. As can be seen from the figure, the laser diode was fiber-coupled to diverging optics that presented a 60 mRad beam. The retroreflected return was collected and directed by the angled flat through a 980nm bandpass filter. The light was then focused onto the cooled avalanche photodiode.

The target platform was equipped with the MRR array, consisting of eight 0.5 mm MQW modulating retroreflectors. Each individual MRR has a mass of about 10 grams (including the holder) and draws about 75 mW of power. The units were driven with 15V which was sufficient to achieve 3:1 optical on/off modulation. Photographs of the hardware resident on the pursuer and target platforms are shown in Figure 9.

Each target MRR was driven by a unique code that was detected, isolated, demodulated, and transformed into an intensity level for use by the acquisition and tracking logic. The eight Gold codes used to modulate the MRR units are shown in Figure 10. Upon performing a search and detect scanning profile with the gimbaled laser system, the eight codes were detected and acquired. This search, detection, and acquisition profile is depicted in Figure 11, wherein the three outer MRR return intensities were equalized once lock-on of the entire array was achieved. The intensity levels from each MRR were then processed by the computer to determine the 5-state relative navigation solution and

subsequently activate simple proportional/derivative closed-loop control logic to perform both initial alignment to the target platform as well as target tracking. A block diagram of the position and attitude controller is provided in Figure 12. The pursuer rate and velocity feedback signals were derived from the motion of the platform rather than directly measured, though an actual spacecraft would likely utilize gyros and accelerometers to provide this information. Additionally, the current system does not include appropriate timing electronics necessary to determine accurate TOF ranging, so we incorporated range measurements derived from the encoder information on each platform trolley system. Future facility upgrades will include the TOF ranging electronics.

As depicted in Figure 13, two closed-loop relative navigation and control tests were performed. The first test consisted of alignment of the pursuer platform frame to a stationary target frame with a commanded 10-meter offset along the platform x-axis. That is, the pursuer was to find the nonmoving target and maintain a LOS link at a 10 meter range.

The second test consisted of a tracking maneuver in which the pursuer platform was commanded to maintain the 10-meter offset alignment to the target while the target moved. The targe traversed a circular 5-meter radius, 30-degree arc in the horizontal plane and then reversed direction to return to its initial location. The tracker was to acquire, track, and maintain link throughout the maneuvers.

Results

Results from both maneuvers are provided in Figures 14 and 15. In each figure the three-axis position error, the two-axis attitude error, and the two gimbal angles are given. It is observed in Figure 14 that an initial position error of 9 meters (primarily along the x-axis) was removed within 6 minutes and an initial attitude error of 5 degrees was removed within 2 minutes. In Figure 15 it is observed that tracking errors occurred while the target was in motion, with the two large position error spikes due to target motion reversal. Of course, these tracking errors are highly dependent on the feedback gains chosen for the tracking controller. For both tests, the steady-state 1-sigma tracking control errors were about 1 cm in position and 0.3 deg in orientation. These values are a function of limits of the hardware, not the technique.

To obtain a quantitative measure of the sensor accuracy for measuring relative orientation of the target (in the absence of control errors), we also performed a static test in which the target and pursuer were aligned and held motionless. Figure 16 shows a plot of the resulting two-axis attitude error, where it is observed that this sensor can potentially provide at least an arcminute-level attitude knowledge accuracy.

Conclusions and Further Research Efforts

We have designed, developed, and experimentally verified a novel dual-use sensor for simultaneous inter-spacecraft optical communication and navigation. The optical communication link from the target to the pursuer is established by illuminating a target platform with a laser beam from an interrogating pursuer platform. The beam illuminates an array of retromodulators which are uniquely coded to provide return signatures to the pursuer craft. Use of the NRL Multiple Quantum Well corner cube retromodulators enables the target array to be populated with devices that require milliwatts, are compact, grams in density, and radiation hard. This technique was demonstrated by uniquely coding eight retromodualtors at a rate of 1 Mbps.

The target's relative position vector and aspect (tilt) angles are derived from the relative intensities of the modulated signal returns from each of retroreflectors on a target array board. Signal discrimination is achieved by passing the aggregate photon return through a set of matching filters tuned to each unique reflector modulation code.

Experimental results using a dual-platform dynamic testbed have demonstrated and verified the concept. Initial alignment to a stationary target and alignment maintenance with respect to a moving target have been successfully demonstrated over a range of 10 to 20 meters, though the concept is valid for ranges up to tens of kilometers provided sufficient laser power is available. The results show promise for applications such as autonomous rendezvous and capture, spacecraft formation flying, and free-flying space interferometry. Future research efforts will encompass further characterization of sensor noise levels and biases, sensitivity to target relative motion, inclusion of time-of-flight target ranging electronics, and inclusion of adaptive optics for range-independent acquisition and track.

References

1. Polites, M. E., "Technology of Automated Rendezvous and Capture in Space," Journal of Spacecraft and Rockets, **36**(2), pp. 280-291 (1999),

2. Creamer, G., "Spacecraft Attitude Determination Using Gyros and Quaternion Measurements," The Journal of the Astronautical Sciences, **44**(3), pp. 357-371, (1996).

3. Junkins, J. L., Hughes, D., Wazni, K., and Pariyapong, V., "Vision-Based Navigation for Rendezvous, Docking, and Proximity Operations," 22nd Annual AAS Guidance and Control Conference, Breckenridge, CO, Feb. 3-7, 1999.

4. Mokuno, M., Kawano, I., and Kasai, T., "Experimental Results of Autonomous Rendezvous Docking on Japanese ETS-VII Satellite," 22nd Annual AAS Guidance and Control Conference, Breckenridge, CO, Feb. 3-7, 1999.

5. D'Souza, C., Bognar, A., and Brand, T., "An Evaluation of the GPS Relative Navigation System for ETS-VII and HTV," 22nd Annual AAS Guidance and Control Conference, Breckenridge, CO, Feb. 3-7, 1999.

6. Cislaghi, M., Fehse, W., Paris, D., and Ankerson, F., "The ATV Rendezvous Predevelopment Programme (ARP)," 22nd Annual AAS Guidance and Control Conference, Breckenridge, CO, Feb. 3-7, 1999.

7. Howard, R. T., Bryan, T. C., Book, M. L., and Dabney, R. W., "The Video Guidance Sensor – A Flight Proven Technology," 22nd Annual AAS Guidance and Control Conference, Breckenridge, CO, Feb. 3-7, 1999.

8. Cruzen, C. A., Lomas, J. J., and Dabney, R. W., "Test Results for the Automated Rendezvous and Capture System," 23nd Annual AAS Guidance and Control Conference, Breckenridge, CO, Feb. 2-6, 2000.

9. Hollander, S., "Autonomous Space Robotics: Enabling Technologies for Advanced Space Platforms," Space 2000 Conference and Exposition, Long Beach, CA, Sept. 19-21, 2000.

10. Purcell, G., Kuang, D., Lichten, S., Wu, S. C., and Young, L., "Autonomous Formation Flyer (AFF) Sensor Technology Development," 21st Annual AAS Guidance and Control Conference, Breckenridge, CO, Feb. 4-8, 1998.

11. Gilbreath, G. C., Bowman, S. R., Rabinovich, W. S., Merk, C. H., and Senasack, H. E., "Modulating Retroreflector Using Multiple Quantum Well Technology," **U. S. Patent No. 6,154,299**, awarded November, 2000.

12. Gilbreath, G. C., et al., "Large Aperture Multiple quantum Well Modulating Retroreflector for Free-Space Optical Data Transfer on Unmanned Aerial Vehicles", Optical Engineering, **40**(7), pp. 1348-1356, July, 2001.

13. Katzer, D. S., Rabinovich, W. S., Ikossi-Anastasiou, K., and Gilbreath, G. C., "Optimization of Buffer Layers for InGaAs/AlGaAs PIN Optical Modulators Grown on GaAs Substrates by Molecular Beam Epitaxy," Journal of Vacuum Science Technology, **B 18**, pp. 1609-1613, (2000).

14. Goetz, P. G., et al., "Effects of Proton Irradiation on InGaAs/AlGaAs Multiple Quantum Well Modulators," IEEE Aerospace Conference, **Paper No. 5.0402**, March, 2001.

15. Gilbreath, G. C., et. al., "Realtime Video Transfer using Multiple Quantum Well Retromodulators", Proceedings of the SPIE, Paper No. **4821-61**, July, 2002.

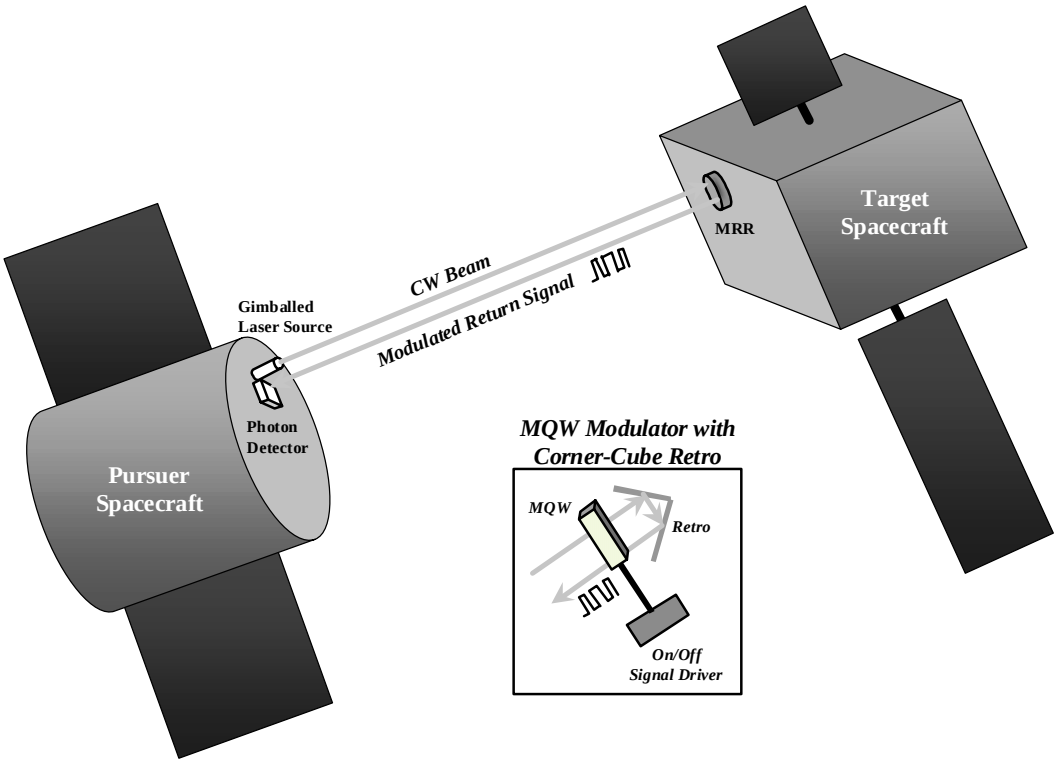

Figure 1. Conceptual depiction of inter-spacecraft communication using modulating retroreflectors.

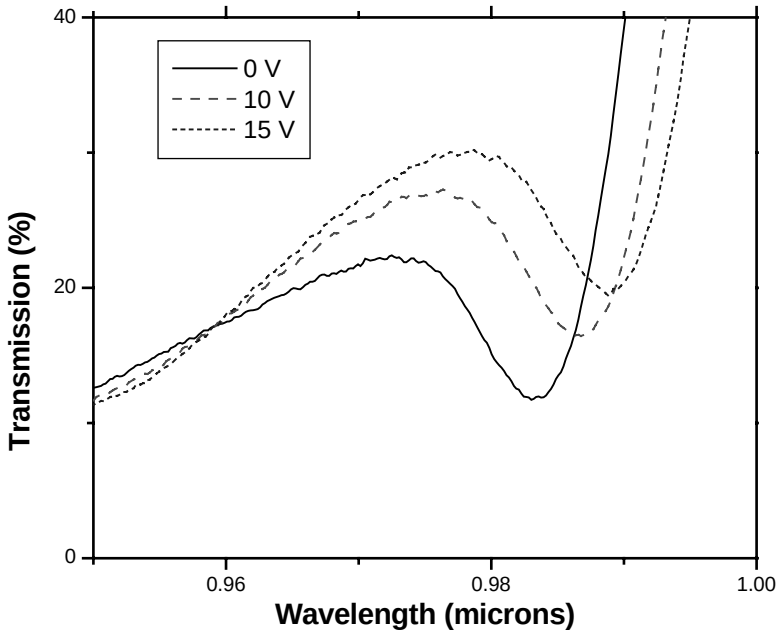

Figure 2. Switching characteristics of an InGaAs-Based MQW modulator.

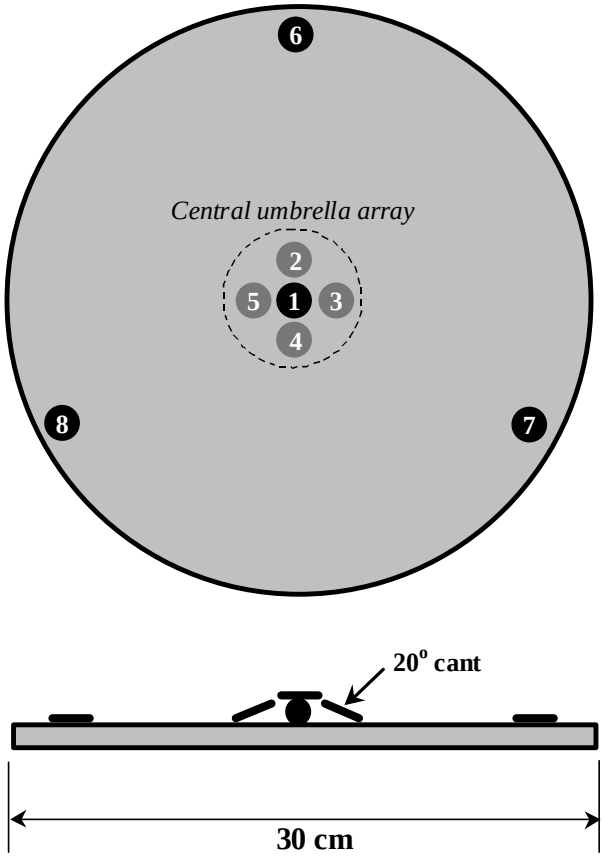

Figure 3. Target MRR array.

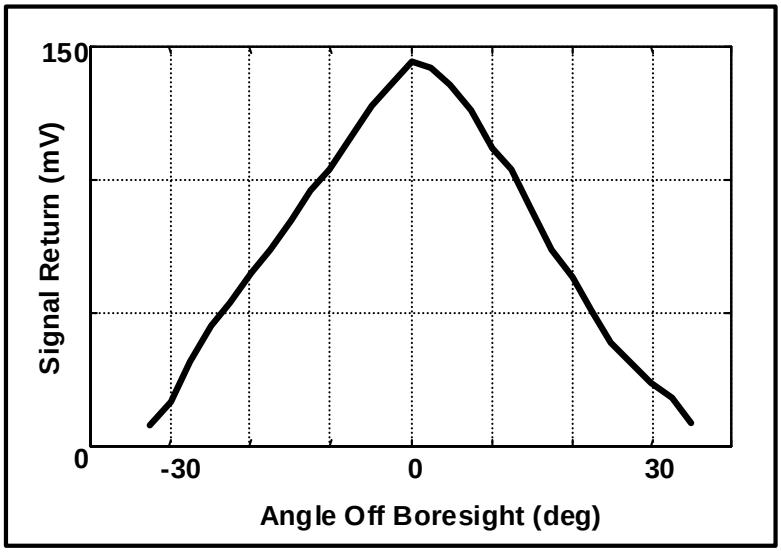

Figure 4. Sensitivity of MRR signal intensity to off-boresight illumination.

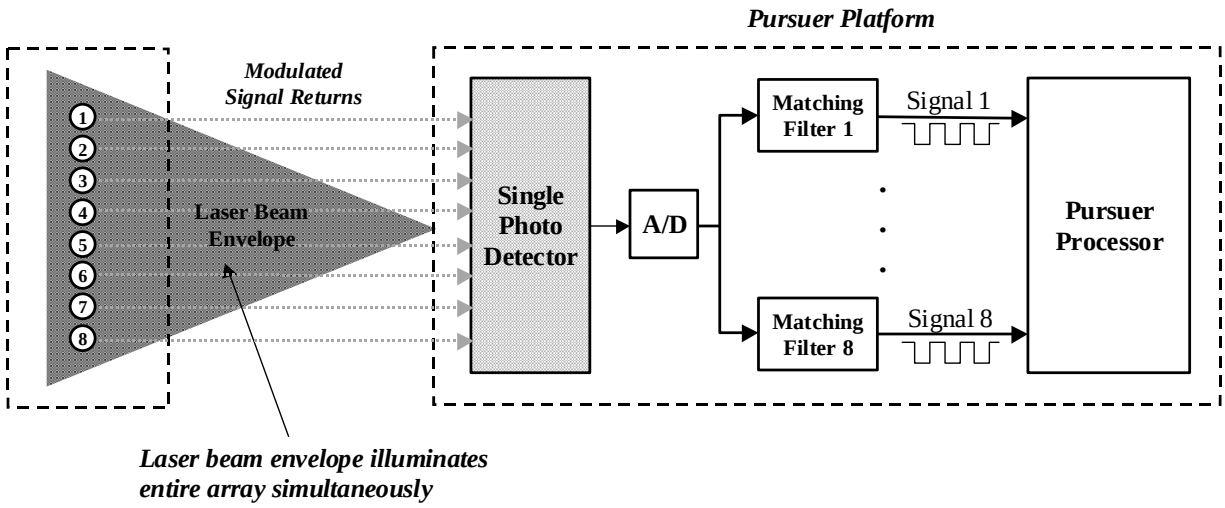

Figure 5. Target-to-pursuer communication and MRR discrimination approach.

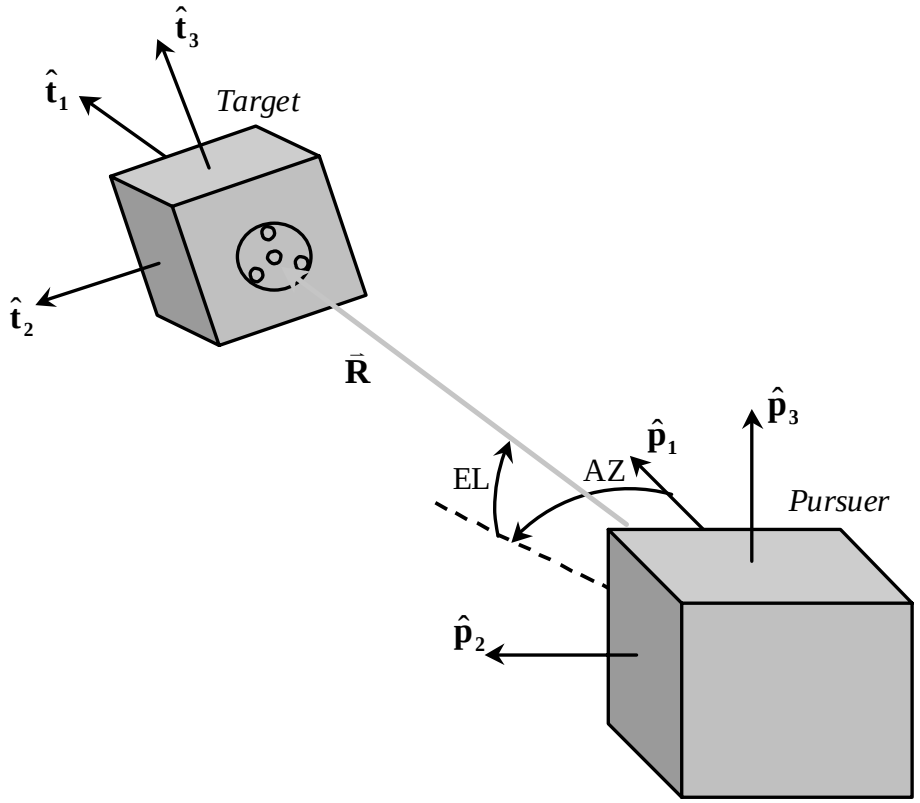

Figure 6. Geometry for inter-spacecraft relative navigation.

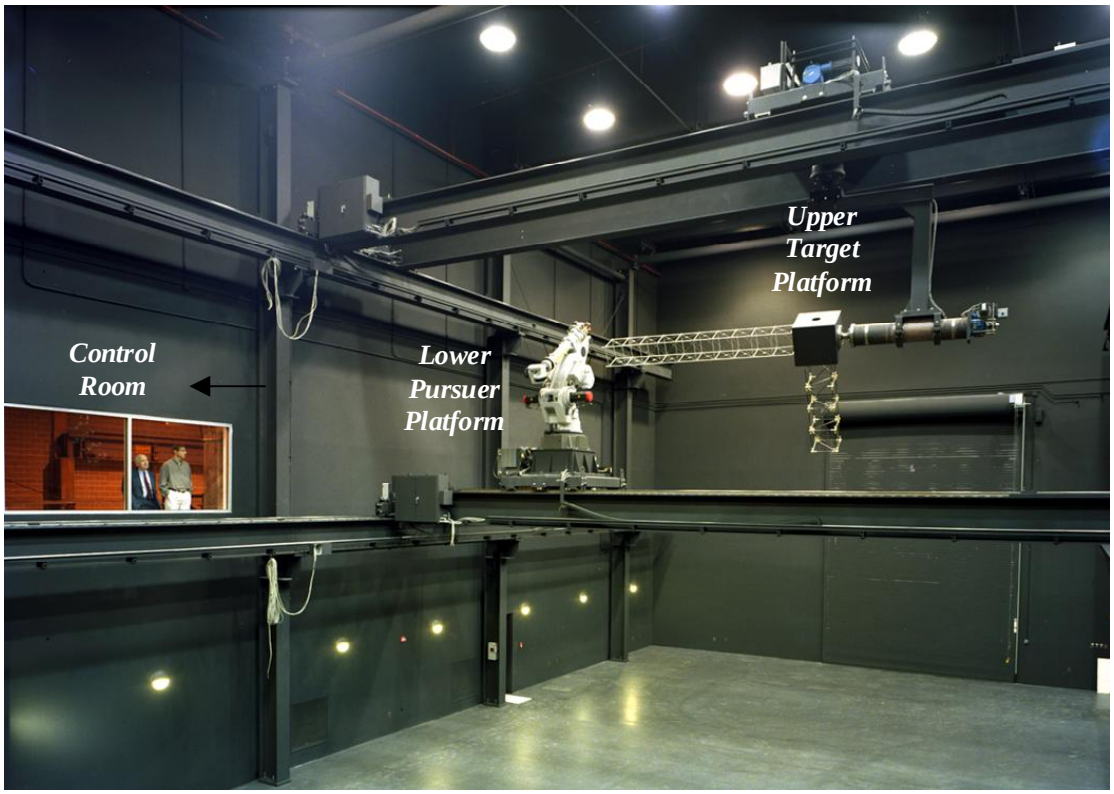

Figure 7. NRL's dual-platform Dynamic Motion Simulator in the Robotics Laboratory.

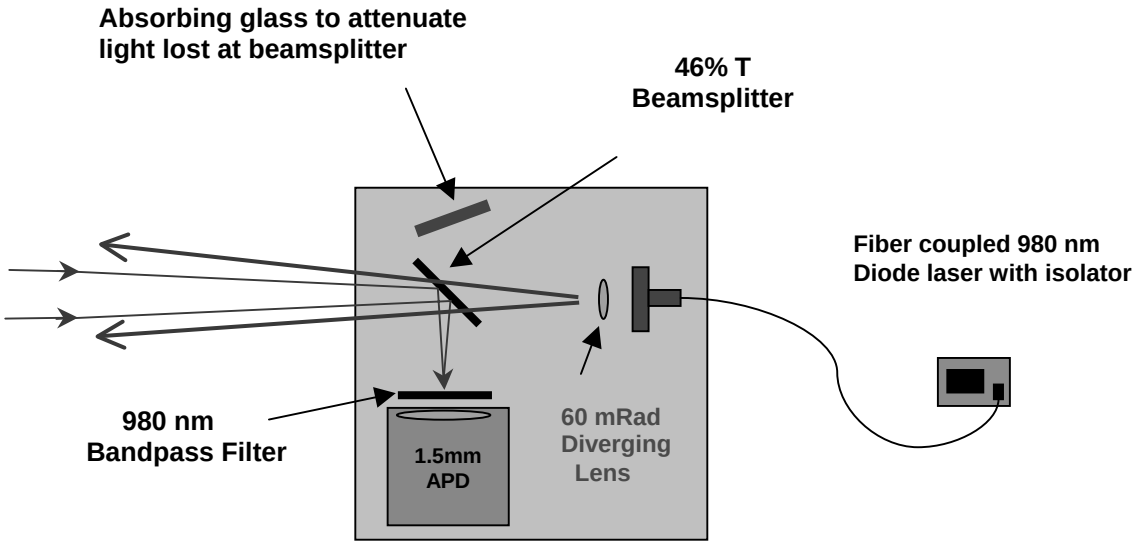

Figure 8. Optical Configuration used on pursuer platform to illuminate target array on target and receive signals from uniquely coded MRR devices.

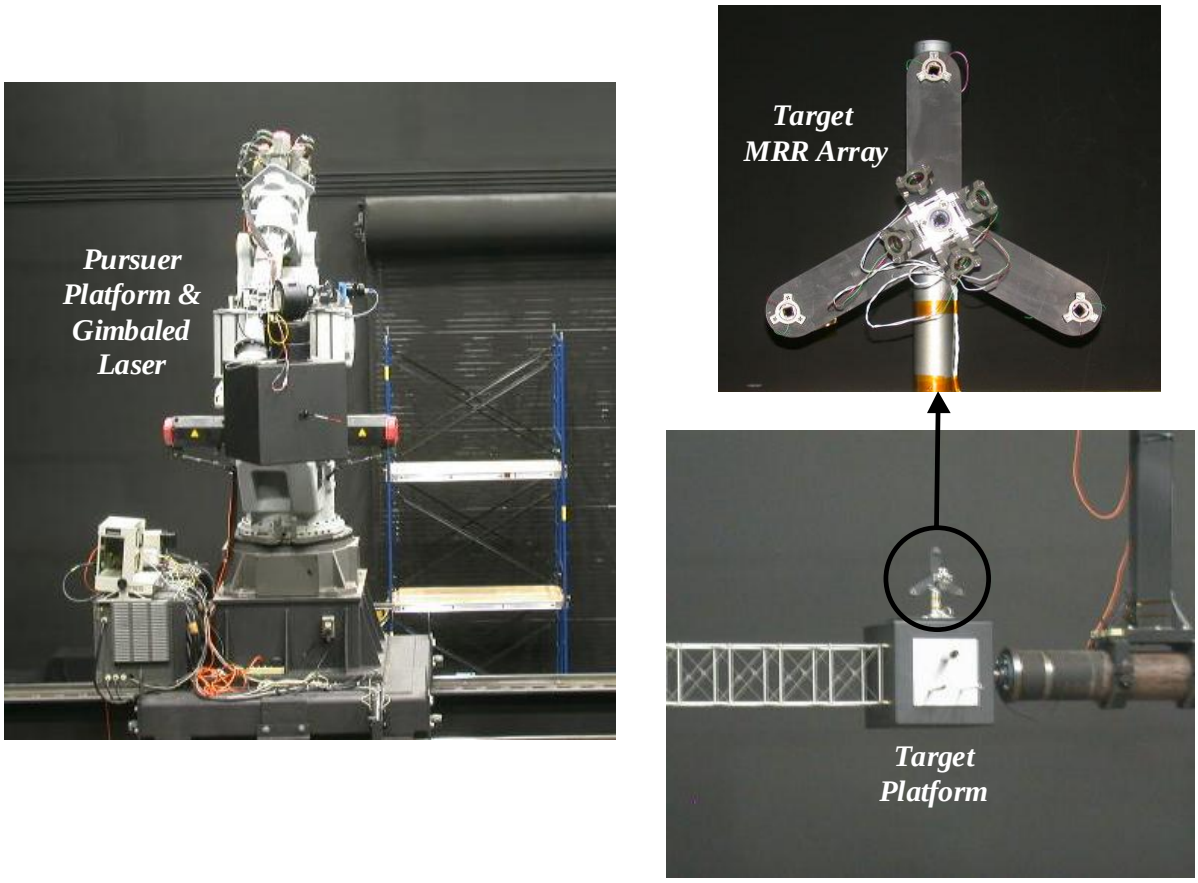

Figure 9. Pursuer and target platform hardware.

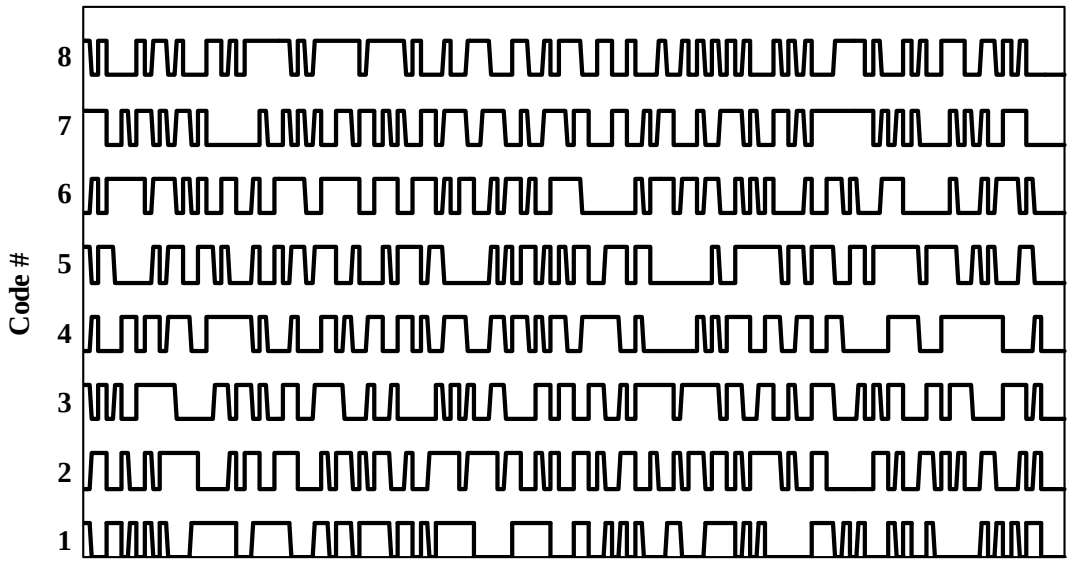

Figure 10. Eight unique MRR code sequences used to identify which device is illuminated.

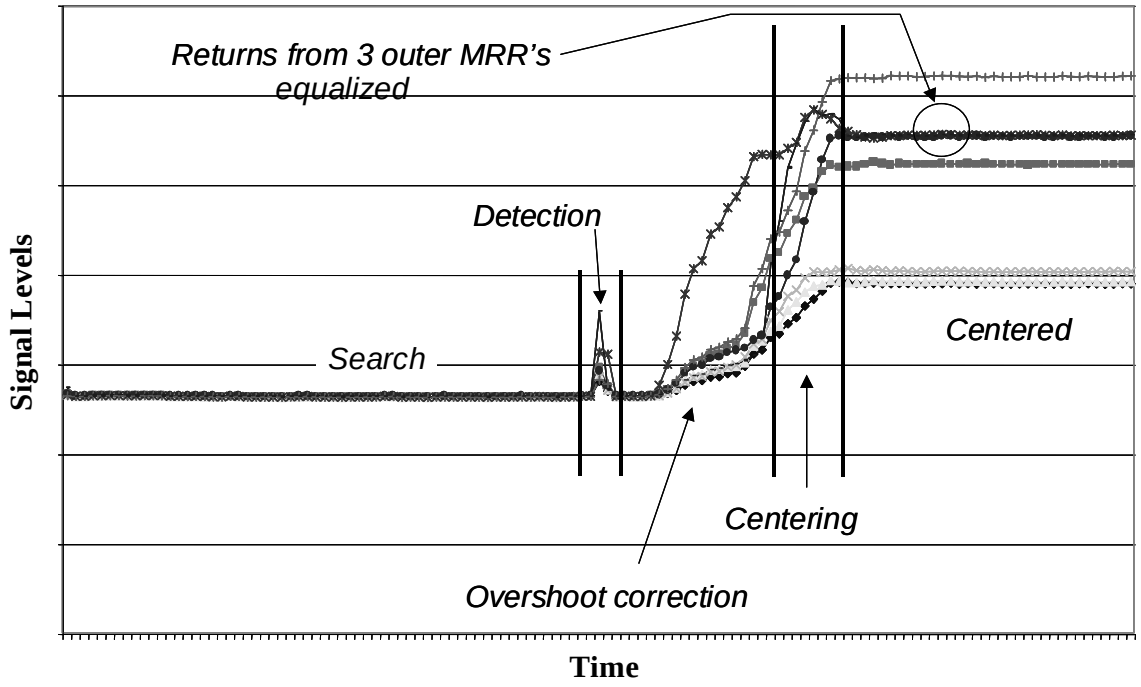

Figure 11. Typical gimbaled laser search, detection, and acquisition of target MRR array.

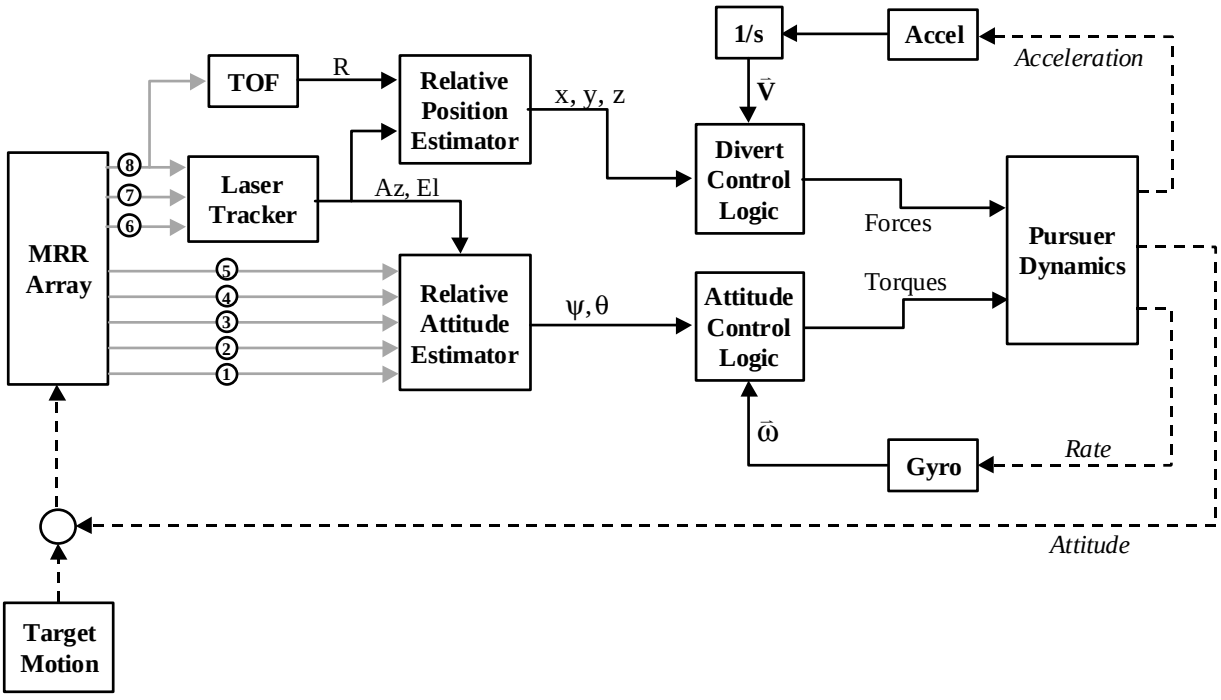

Figure 12. Pursuer tracking control block diagram.

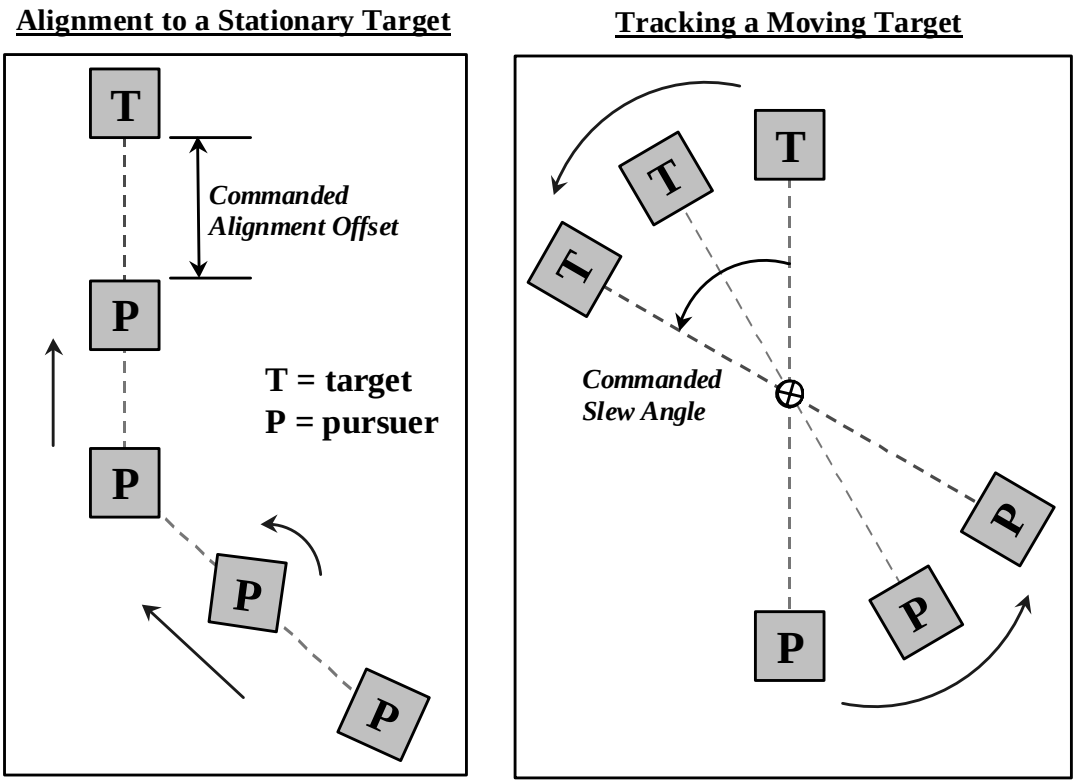

Figure 13. Two closed-loop tests used for concept verification and performance evaluation.

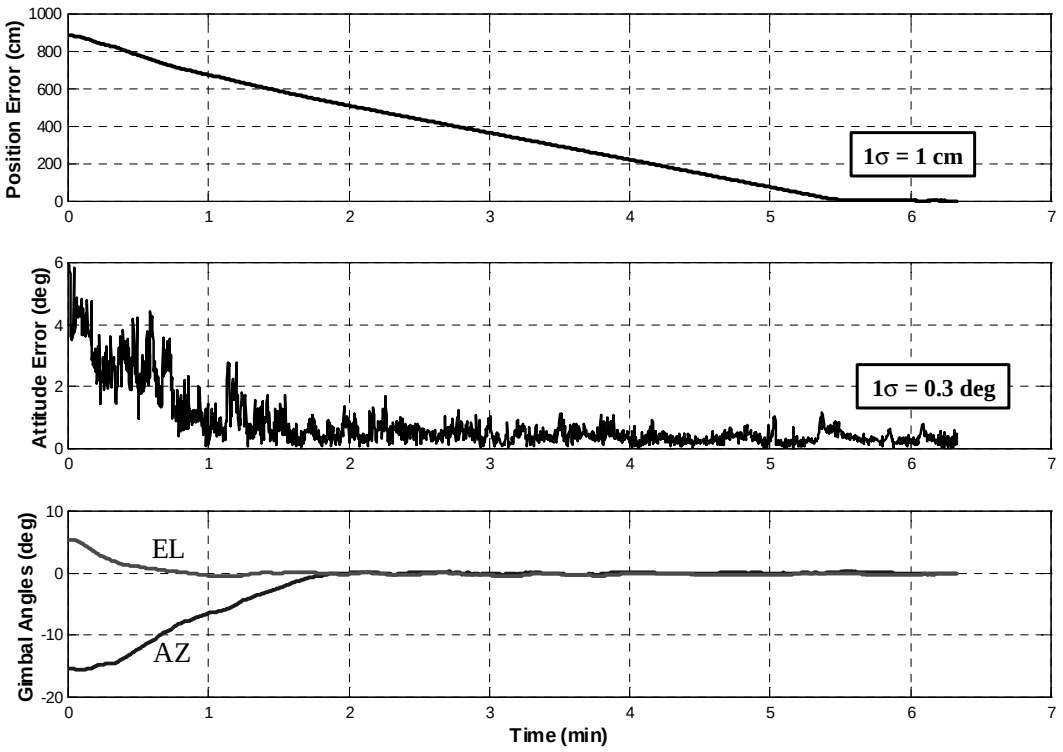

Figure 14. Experimental results for alignment to a stationary target.

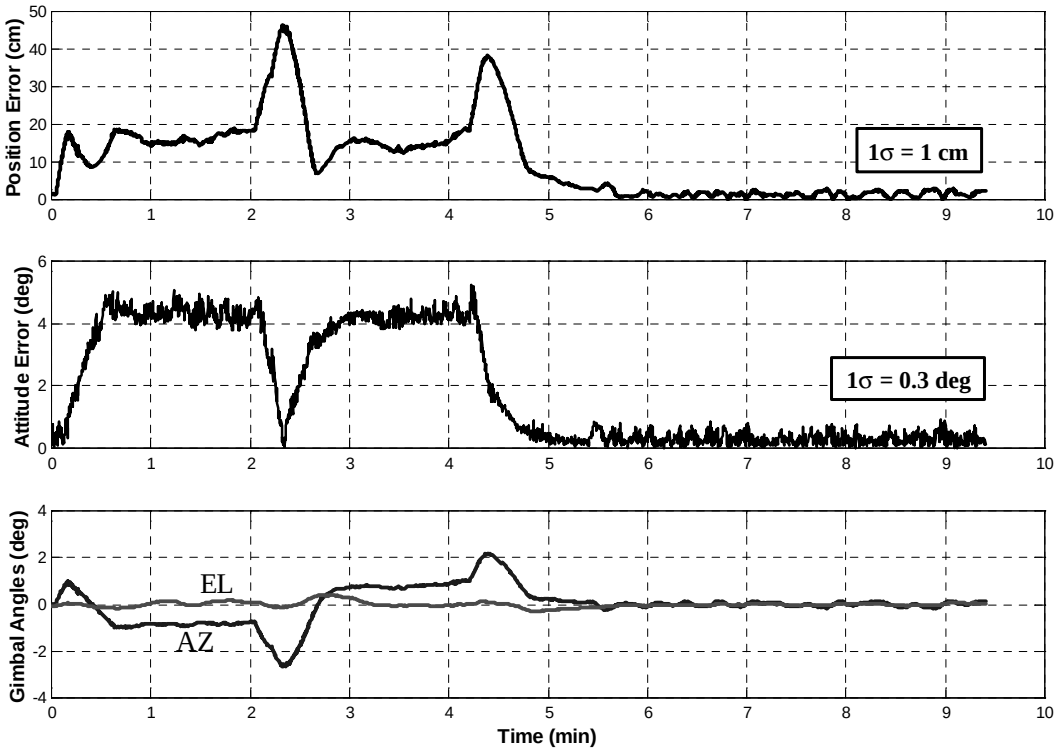

Figure 15. Experimental results for tracking a moving target.

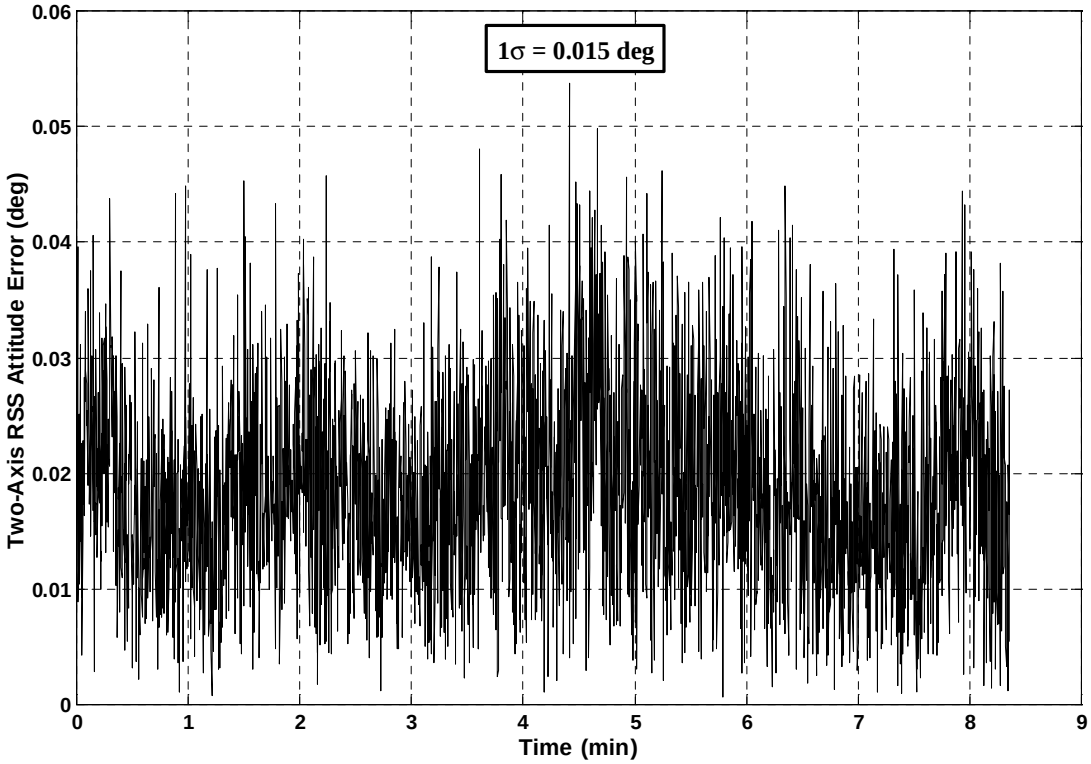

Figure 16. Experimental results for stationary attitude estimation.